# The Rubisco Chaperone BSD2 May Regulate Chloroplast Coverage in Maize Bundle Sheath Cells[1][OPEN]

**Coralie Salesse,[a] Robert Sharwood,[b] Wataru Sakamoto,[c] and David Stern[a,2]**

[a]Boyce Thompson Institute, Cornell University, Ithaca, New York 14853
[b]Research School of Biology, Australian National University, Canberra, Australian Capital Territory 0200, Australia
[c]Institute of Plant Science and Resources, Okayama University, Kurashiki, Okayama 710-0046, Japan

**ORCID IDs: 0000-0002-2856-4217 (C.S.); 0000-0003-4993-3816 (R.S.); 0000-0001-9747-5042 (W.S.); 0000-0002-0653-6602 (D.S.).**

In maize (*Zea mays*), Bundle Sheath Defective2 (BSD2) plays an essential role in Rubisco biogenesis and is required for correct bundle sheath (BS) cell differentiation. Yet, BSD2 RNA and protein levels are similar in mesophyll (M) and BS chloroplasts, although Rubisco accumulates only in BS chloroplasts. This raises the possibility of additional BSD2 roles in cell development. To test this hypothesis, transgenic lines were created that overexpress and underexpress BSD2 in both BS and M cells, driven by the cell type-specific Rubisco Small Subunit (RBCS) or Phosphoenolpyruvate Carboxylase (PEPC) promoters or the ubiquitin promoter. Genetic crosses showed that each of the transgenes could complement Rubisco deficiency and seedling lethality conferred by the *bsd2* mutation. This was unexpected, as RBCS-BSD2 lines lacked BSD2 in M chloroplasts and PEPC-BSD2 lines expressed half the wild-type BSD2 level in BS chloroplasts. We conclude that BSD2 does not play a vital role in M cells and that BS BSD2 is in excess of requirements for Rubisco accumulation. BSD2 levels did affect chloroplast coverage in BS cells. In PEPC-BSD2 lines, chloroplast coverage decreased 30% to 50%, whereas lines with increased BSD2 content exhibited a 25% increase. This suggests that BSD2 has an ancillary role in BS cells related to chloroplast size. Gas exchange showed decreased photosynthetic rates in PEPC-BSD2 lines despite restored Rubisco function, correlating with reduced chloroplast coverage and pointing to $CO_2$ diffusion changes. Conversely, increased chloroplast coverage did not result in increased Rubisco abundance or photosynthetic rates. This suggests another limitation beyond chloroplast volume, most likely Rubisco biogenesis and/or turnover rates.

Bundle Sheath Defective2 (BSD2) is a small, chloroplast-localized DnaJ-type zinc finger protein, originally identified during a screen for maize (*Zea mays*) mutants with abnormal Kranz anatomy (Roth et al., 1996) and further characterized upon isolation of the defective gene (Brutnell et al., 1999). The maize *bsd2* mutant is unable to develop normal bundle sheath (BS) chloroplasts or accumulate Rubisco, resulting in seedling lethality. It is not yet clear whether the abnormal BS phenotype drives lower Rubisco accumulation, the BS phenotype is a pleiotropic effect of Rubisco loss, or if in fact BSD2 confers two independent functions.

BSD2 does not appear to impact transcription or translation of the Rubisco subunit genes, apart from an increased accumulation of *rbcL* transcripts in mesophyll (M) cells (Roth et al., 1996). Based on available evidence, BSD2 was proposed to interact with the large subunit (LS) of Rubisco to facilitate its translation and/or folding (Brutnell et al., 1999). Subsequent work in maize showed that BSD2 likely interacts with nascent LS and/or newly imported small subunit as well as other assembly factors (RAF1 and RAF2) to assemble the Rubisco holoenzyme (Feiz et al., 2012, 2014). More limited data are consistent with analogous roles in *Nicotiana benthamiana* (Wostrikoff and Stern, 2007) and *Chlamydomonas reinhardtii* (Doron et al., 2014).

A hint that BSD2 may have a role apart from Rubisco biogenesis came from quantitative proteomics showing that BSD2 accumulates at equivalent levels in maize BS and M chloroplasts (Friso et al., 2010). This finding challenges the presumption of a specific role of BSD2 in Rubisco regulation, since Rubisco does not accumulate in M chloroplasts. One possibility is that BSD2 is involved in repressing LS translation in M chloroplasts through a phenomenon known as control by epistasy of synthesis (Choquet and Wollman, 2009). In the case of Rubisco, unassembled LS undergoes translational repression through direct or indirect interaction with the *rbcL* transcript (Wostrikoff and Stern, 2007). Thus, a potential role of BSD2 in M chloroplasts could be to promote the folding of enough LS to exert a negative autoregulatory effect. Indeed, M *rbcL* transcripts are

[1] This material is based upon work that is supported by the Agriculture and Food Research Initiative from the National Institute of Food and Agriculture, U.S. Department of Agriculture, under award number 2016-67013-24464.

[2] Address correspondence to ds28@cornell.edu.

The author responsible for distribution of materials integral to the findings presented in this article in accordance with the policy described in the Instructions for Authors (www.plantphysiol.org) is: David Stern (ds28@cornell.edu).

C.S. and D.S. designed the study; C.S., R.S., and W.S. performed research and analyzed data; C.S. and D.S. wrote the article; all authors read and reviewed the final article.

[OPEN] Articles can be viewed without a subscription.
www.plantphysiol.org/cgi/doi/10.1104/pp.17.01346

 

released from translational arrest in the *bsd2* mutant (Brutnell et al., 1999).

To test this hypothesis, and to uncover any other additional functions of BSD2 in maize, we created transgenic lines designed to overexpress or underexpress BSD2 in either BS and M cells using different promoter-*BSD2* fusions. While we could not substantiate a role of BSD2 in M translational regulation, we found that the level of BSD2 expression in BS, but not M, cells could be correlated with chloroplast coverage (i.e. the proportional cellular area occupied by chloroplasts). Furthermore, lines with smaller chloroplasts had lesser photosynthetic rates, possibly due to alterations in $CO_2$ diffusion between the BS and M cells. However, lines with larger chloroplasts did not have improved photosynthetic rates, indicating that Rubisco remains the rate-limiting step in $CO_2$ assimilation. These results reveal that BSD2 may link Rubisco biogenesis to chloroplast coverage in BS cells.

## RESULTS

### Creation of Transgenic Lines and Complementation of the Maize *bsd2* Mutant

To differentiate the roles of BSD2 in M and BS chloroplasts, we created the three constructs shown in Figure 1A. Each construct contained the *BSD2* coding sequence with a C-terminal FLAG tag preceded by a different promoter. The promoters were derived from the maize *UBI*, *RbcS*, and *PEPC* genes, and their expression domains were defined previously using promoter-YFP fusions (Sattarzadeh et al., 2010). The *UBI* promoter is highly expressed in both M and BS cells, whereas *RbcS* promoter activity is restricted to BS cells. When YFP was expressed from the *PEPC* promoter, most of the fluorescence was in the M; however, confocal microscopy and protoplast purification showed leaky expression in BS cells. Therefore, the PEPC-BSD2 fusion was expected to express in both cell types, albeit primarily in the M. To fine-tune the BS component of that expression, we studied both hemizygous and homozygous lines for this transgene.

Each transgene was stably introduced into Hi-II maize, and single-insertion, nonsilencing events were propagated. To discover whether the transgenes could complement the *bsd2* mutation, transgenic plants were crossed to *bsd2* heterozygotes, as the homozygote mutant is seedling lethal. Transgene-expressing *bsd2* heterozygotes resulting from those crosses were selfed, and healthy green progeny were genotyped for the *bsd2* mutation, which is caused by a *Mu* transposon insertion (Supplemental Fig. S1). In each case, plants were found that were homozygous for the *bsd2* mutation yet able to grow normally (Fig. 1B) and produce seed. Thus, each of the transgenes could complement the seedling lethality of the *bsd2* mutation.

Complementation by UBI-BSD2 was expected, since that promoter expresses strongly in most cell types, whereas complementation by the BS-specific RBCS-BSD2 transgene suggested that BSD2 does not have an essential function in M chloroplasts. Complementation

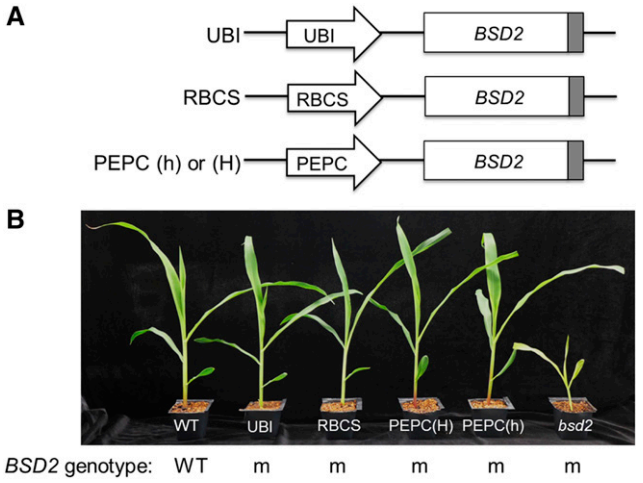


**Figure 1.** Constructs introduced into maize and growth phenotypes of complemented lines. A, Schematics of transgene constructs. The *BSD2* coding region is flanked by a FLAG epitope tag (gray box) and driven by the Ubiuitin (UBI), Rubisco Small Subunit (RbcS), or Phosphoenolpyruvate Carboxylase (PEPC) promoter. The *BSD2* coding region includes an N-terminal chloroplast transit peptide. h indicates hemizygote and H indicates homozygote with respect to transgene copy number. B, Transgenic lines were crossed to heterozygous *bsd2* mutants and self-pollinated to yield homozygous *bsd2* mutants complemented by the transgenes, as shown for 14-d-old plants. m, Mutant; WT, wild type.

by PEPC-BSD2 was surprising, because PEPC-YFP fusions are poorly expressed in BS cells and BSD2 is essential for Rubisco assembly, which takes place in that cell type. Therefore, we obtained quantitative estimates for BSD2 expression in each of the transgenic lines.

### PEPC-BSD2 Complemented Lines Accumulate Reduced BSD2 in the BS But Retain Wild-Type Levels of Rubisco

To assess transgene expression, protein was extracted from total leaf tissue, BS, and M cells (Fig. 2). As shown in Figure 2A for total leaf protein, BSD2 accumulates at a higher than wild-type level in all the transgenic lines. This is because each of the transgene promoters is stronger than the native *BSD2* promoter. When the hemizygous PEPC-BSD2 line was compared with the homozygous PEPC-BSD2 line, it accumulated approximately half as much BSD2 as might be expected.

M and BS protein preparations were made to determine in which cell types BSD2 was accumulating. Antibodies against PEPC, an M-specific protein, and NADP-ME, a BS-specific protein, were used to assess the purity of the BS and M cell preparations, which was equivalent for all lines tested (Fig. 2, B and C). BSD2 protein was estimated both with an antibody raised against recombinant BSD2 ($\alpha$-BSD2) for the native and tagged proteins together and with anti-FLAG for transgene-encoded BSD2. As expected, the UBI-BSD2 line accumulated a high level of BSD2 in both cell types, whereas the RBCS-BSD2 line displayed highly

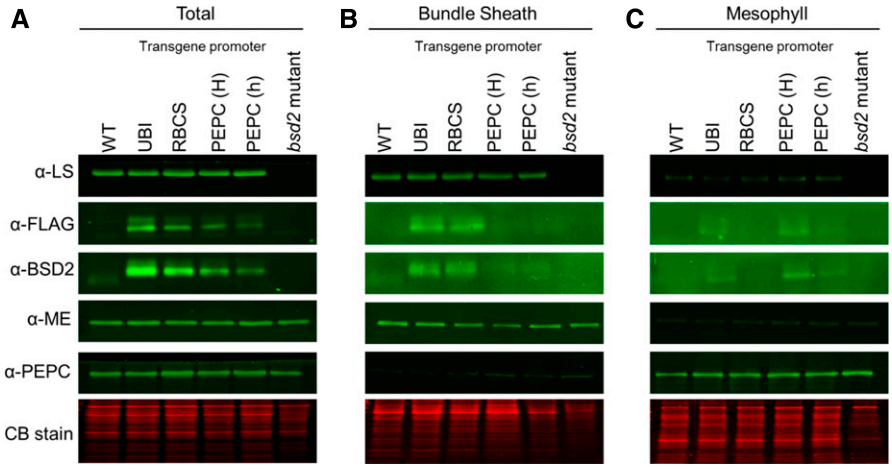


**Figure 2.** Protein accumulation and cell type specificity in transgenic lines. A to C, Soluble protein was isolated from total leaf (A), BS (B), and M (C) preparations and analyzed by immunoblotting using the antibodies indicated at left. α-FLAG recognizes BSD2 expressed from transgenes; α-BSD2 recognizes both endogenous and transgene-encoded BSD2. PEPC and NADP-Malic Enzyme (ME) were used as controls for M and BS cell purity, respectively. Images of the stained gels were vertically compressed and used to reflect loading. Representative blots are shown. CB, Coomassie Blue. D, Quantification of LS and BSD2 protein was achieved using the Odyssey infrared imaging system. The wild-type (WT) level was set to 1 as a baseline. The derived values were based on three biological replicates for LS and two biological replicates for BSD2 ± SE. A second replicate for BSD2 is provided in Supplemental Figure S2.

D

| | Total LS | Total BSD2 | BSD2 (BS) | BSD2 (M) |
|---|---|---|---|---|
| **WT** | 1 | 1 | 1 | 1 |
| **UBI** | 1.11 ±0.05 | 6.96 ±2.34 | 5.26 ±0.33 | 10.5 ±1.25 |
| **RBCS** | 1.17 ±0.06 | 5.10 ±0.03 | 3.88 ±0.22 | 0.65 ±0.21 |
| **PEPC (H)** | 1.14 ±0.11 | 4.59 ±0.89 | 0.37 ±0.02 | 9.55 ±0.73 |
| **PEPC (h)** | 1.17 ±0.06 | 2.70 ±0.53 | 0.36 ±0.01 | 4.24 ±0.45 |
| ***bsd2*** | 0 | 0 | 0 | 0 |

elevated BSD2 in BS, while none was detectable in the M. Both hemizygotic and homozygotic PEPC-BSD2 transgenes confer higher than wild-type BSD2 accumulation in M, with the homozygous line accumulating twice as much BSD2 in the M. Low levels of BSD2 accumulate in BS cells of the PEPC-BSD2 lines at comparable levels due to the leaky expression of the promoter. This leaky expression of the PEPC promoter in BS cells explains why the PEPC-BSD2 transgene can complement the *bsd2* null mutation in terms of restoring seedling viability.

We analyzed the accumulation of Rubisco using an anti-LS antibody. As expected, LS was abundant in all total and BS protein samples and undetectable in all M and *bsd2* mutant samples. There was no correlation between the amount of BSD2 and the amount of Rubisco LS, the latter of which was similar in all lines other than *bsd2* (Fig. 2D, Total LS column). This suggests that overexpression of BSD2 by itself does not confer increased Rubisco content. We can additionally conclude that the C-terminal FLAG tag does not prevent BSD2 from fulfilling its role in Rubisco assembly, although we cannot rule out smaller effects on its activity. We also assessed Rubisco content using [$^{14}$C]CABP binding, which confirmed that wild-type Rubisco levels had been restored in all the complemented lines (see Table II below).

BSD2 accumulation was quantified from PEPC-BSD2 lines using an infrared scanner (Fig. 2D). Because of the low level in both the wild-type and BS preparations from PEPC-BSD2 lines, we used multiple gels and protein preparations (Supplemental Fig. S2) to arrive at the most accurate possible estimate relative to the wild type. We also looked at total BSD2 protein expression in two transgenic events to control for differences that could have been caused by the transgene insertion site (Supplemental Fig. S3). This led to the conclusion that both homozygous and hemizygous PEPC-BSD2 lines contain approximately 50% less BSD2 protein in their BS than do wild-type plants. These same lines, however, accumulate wild-type levels of Rubisco, suggesting that, in wild-type plants, the amount of BSD2 is in excess of what is required for Rubisco accumulation.

### Enhanced *rbcL* Transcript Accumulation Does Not Occur in M Cells of Complemented Plants That Lack Mesophyll BSD2

The transgenic lines allowed us to test the hypothesis that BSD2 is involved in regulating the *rbcL* mRNA level in M cells. This hypothesis arose from the observation that *rbcL* transcripts overaccumulate in M cells of the *bsd2* mutant (Roth et al., 1996). To test whether hemicomplementation by RBCS-BSD2, which lacks BSD2 in the M, would exhibit the same phenotype, RNA gel-blot analysis was performed on total, M, and BS RNA from 2-week-old leaves (Supplemental Fig. S4). On a total RNA basis, no change in *rbcL* transcript accumulation was observed between the transgenic lines and the wild type. Consistent with previous reports, *rbcL* mRNA increased in the M of the *bsd2* mutant (Supplemental Fig. S4, right

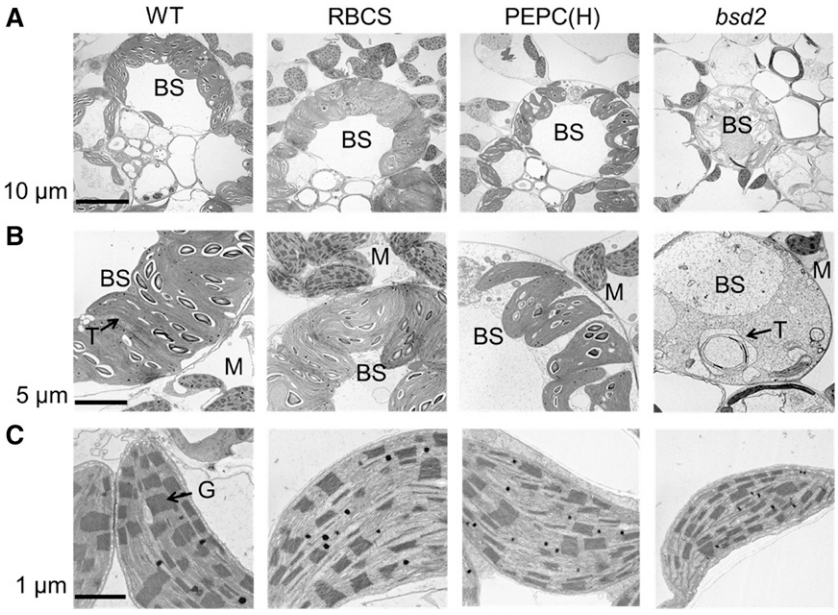


**Figure 3.** Transmission electron microscopy (TEM) images from leaf tip tissue of 11-d-old seedlings. Samples were prepared as described in "Materials and Methods." The top row shows images of BS cells, the middle row shows closeups of BS cells, and the bottom row shows closeups of M cells. G, Grana; T, thylakoid membranes; WT, wild type.

lanes) as well as in total RNA. However, the results showed that *rbcL* transcripts were not increased relative to the wild type in M cell RNA prepared from RBCS-BSD2, signifying that the increased *rbcL* transcript phenotype of *bsd2* is likely a pleiotropic effect of the lack of Rubisco and not the effect of missing BSD2 in the M. The same phenomenon is seen in the maize *raf1* mutant, which is blocked at a similar step in Rubisco assembly to *bsd2* (Feiz et al., 2012). The function of BSD2 in the M remains unclear. Identifying its binding partners through use of the FLAG tag, combined with cell type-specific expression, could shed light on both M function and Rubisco assembly.

### Chloroplast Coverage Is Reduced in BS Cells of the PEPC-BSD2 Complemented Plants

To reveal any changes in cell and chloroplast morphology, transverse leaf sections of 11-d-old seedlings were examined by confocal microscopy (Supplemental Fig. S5) and electron microscopy (Fig. 3). No differences were observed between the M cell chloroplasts of the wild-type and transgenic lines, while *bsd2* mutant chloroplasts appeared smaller, albeit with normal internal structure (Fig. 3C). Normal M chloroplast structure was reported previously in *bsd2* at various developmental stages (Roth et al., 1996).

In BS cells, the *bsd2* mutant exhibited the previously reported breakdown of the thylakoid membranes and swelling in the outer chloroplast membrane (Fig. 3, A and B). BS chloroplast ultrastructure was restored to the wild-type level in the RBCS-BSD2 and homozygous PEPC-BSD2 complemented lines. Differences were observed, however, in chloroplast coverage, defined as the total chloroplast area per cell area. Based on visual inspection, chloroplast coverage appeared to be greater in the RBCS-BSD2 complemented line and reduced in the homozygous PEPC-BSD2 complemented line.

To quantify this parameter, we used digital analysis of multiple TEM and confocal images for each genotype to calculate chloroplast size, BS cell size, and chloroplast number and to derive chloroplast coverage (see "Materials and Methods"). Figure 4A shows that the average chloroplast area (total area of all chloroplasts in a given cell) was significantly greater in the RBCS line and significantly reduced in the PEPC-BSD2 line, relative to the wild type. The number of chloroplasts per BS cell area remained constant between the genotypes, however, indicating that the increase in chloroplast area was not due to an increased chloroplast count (Fig. 4B). We then derived chloroplast coverage, which closely tracked the results for chloroplast area, revealing that the differences in chloroplast area appear to represent a change in chloroplast size (Fig. 4C). Chloroplast coverage of each genotype also remained consistent between multiple transgenic events (Supplemental Fig. S6). These trends correlate with the relative amount of BSD2 protein found in BS cells, indicating that BSD2 may play a role in determining BS chloroplast area. We cannot rule out an effect of BSD2 overexpression in M cells of the PEPC-BSD2 complemented lines that is manifested in BS cells; however, this is rather unlikely to be the case, as the UBI line, which also overexpressed BSD2 in M cells, does not exhibit the same phenotype.

### PEPC-BSD2 Complemented Lines Have Reduced $CO_2$ Fixation

The variation observed in chloroplast coverage prompted us to ask whether chloroplast coverage could be correlated with photosynthetic rate. To do so, carbon

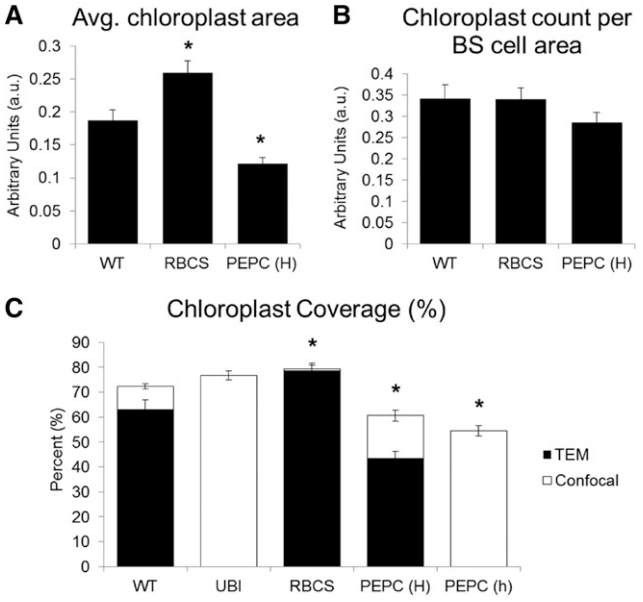


**Figure 4.** Quantification of chloroplast area and coverage in BS cells. A, Comparison of average chloroplast area in the transgenic lines relative to the wild type (WT). Data represent averages of at least 10 leaf sections ± SE. Statistical significance tests were conducted using a one-way ANOVA (*, $P > 0.05$). B, Average number of chloroplasts per BS cell normalized to cell area. Data replicates and analysis were as for A. C, Percentage chloroplast coverage calculated from total chloroplast area divided by BS cell area. White bars represent areas quantified from confocal images, and black bars represent areas quantified from TEM images. Data replicates and analysis were as for A for TEM, while the confocal data represent averages of at least 20 leaf sections ± SE.

fixation measurements were made on the youngest fully expanded leaves of 2-week-old plants. As shown in Figure 5, light-response curves showed no significant difference in light-saturated photosynthesis rates between the wild-type, UBI-BSD2, and RBCS-BSD2 lines, while, as expected, the *bsd2* mutant was unable to successfully incorporate $CO_2$ (Fig. 5A). Thus, increased chloroplast coverage in the RBCS-BSD2 line did not confer additional $CO_2$ assimilation under these conditions. On the other hand, reduced chloroplast coverage in the homozygous PEPC-BSD2 line did correlate with a nearly 50% reduction in photosynthetic rate, even at medium light intensity (greater than 500 $\mu$mol photons $m^{-2}$ $s^{-1}$). Decreased photosynthetic efficiency also was seen at lower light intensities, indicating a limitation in the conversion of light energy into ATP and NADPH. A similar trend, but with reduced magnitude, was seen with $CO_2$-response curves, while the wild-type, UBI-BSD2, and RBCS-BSD2 lines were indistinguishable (Fig. 5B). Specifically, the homozygous and hemizygous PEPC-BSD2 lines displayed photosynthetic rates 20% to 25% less than the wild type at a saturating $CO_2$ concentration (greater than 200 $\mu$mol $mol^{-1}$). Similar results were obtained with the analysis of a second transgenic event (Supplemental Fig. S6). The failure of the PEPC-BSD2 lines to incorporate $CO_2$ normally, even while they accumulate wild-type levels of Rubisco, raised the possibility that reduced chloroplast coverage impacts photosynthetic capacity.

Due to the tight link between the light and light-independent reactions of photosynthesis, decreased carbon fixation might, in turn, decrease the rate of consumption of light reaction products (ATP and NADPH), lowering PSII efficiency (Kramer and Evans, 2011). To assess the light reactions, pulse amplitude fluorometry was used to measure the light intensity dependence of PSII operating efficiency (ΦPSII) and nonphotochemical quenching (NPQ), as shown in Figure 6. ΦPSII is the efficiency at which light absorbed by the PSII complex is used for photosynthesis, essentially a measure of linear electron transport. Figure 6A shows that ΦPSII decreased significantly in the *bsd2* mutant, consistent with the PSII complex being severely damaged. The other lines did not differ from the wild type, except that the homozygous PEPC-BSD2 line had a 32% decrease in PSII efficiency at high light (PAR of 1,500 $\mu$mol photons $m^{-2}$ $s^{-1}$), consistent with its lower photosynthetic efficiency (Fig. 5A) and carbon assimilation rate (Fig. 5B).

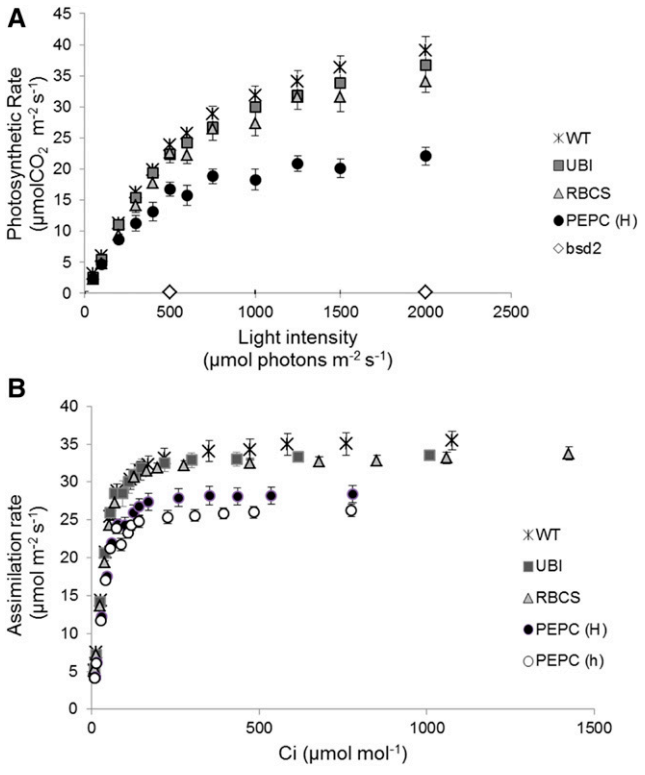


**Figure 5.** $CO_2$ assimilation measurements with varying light intensity and intercellular $CO_2$ partial pressure ($C_i$). A, Responses in the rate of carbon fixation relative to light intensity measured at 400 $\mu$L $L^{-1}$ $CO_2$ and a temperature of 25°C. Data points are averages of at least three replicates ± SE. Statistical significance tests were conducted on data measured at PAR of 1,500 $\mu$mol photons $m^{-2}$ $s^{-1}$ using a one-way ANOVA ($P > 0.05$). Note that both PEPC-BSD2 (H) and (h) are significantly different from the wild type. B, Responses in the rate of carbon fixation relative to intercellular $CO_2$ concentration measured at a light intensity of 1,800 $\mu$mol $m^{-2}$ $s^{-1}$ and a temperature of 25°C. Data points are averages of at least three replicates ± SE. WT, Wild type.

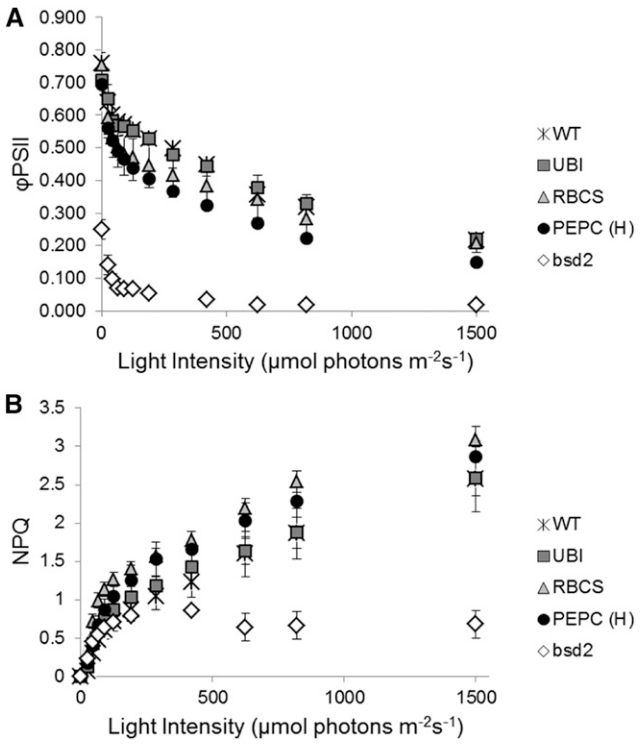


**Figure 6.** Determination of photosynthetic capacity using fluorescence imaging. A, Light intensity dependence of ΦPSII. Measurements were made on attached leaves after they were dark adapted for at least 15 min at room temperature. Values represent averages of at least three replicates ± SE. Statistical significance tests were conducted on data measured at PAR of 1,500 $\mu$mol photons $m^{-2}$ $s^{-1}$ using a one-way ANOVA ($P > 0.05$). B, Light intensity dependence of NPQ. Measurements were made as described for A. WT, Wild type.

NPQ represents photoprotective dissipation of excess absorbed light energy as heat. In lines where PSII efficiency is lowered, NPQ should increase to lower the excitation of PSII and avoid oxidative damage. As shown in Figure 6B, NPQ decreases in the *bsd2* mutant, indicating deficiency of the protective function. The homozygous PEPC-BSD2 line had a slight increase in NPQ, in keeping with lower PSII efficiency. Finally, we determined $F_v/F_m$ ratios, which represent the maximum efficiency at which light absorbed by PSII is used for photosynthesis (Table I). Stressed plants have lower $F_v/F_m$ ratios, as seen in the *bsd2* mutant. All other lines had $F_v/F_m$ ratios of ~0.7 to 0.8, in the normal range (Maxwell and Johnson, 2000). Together, these results suggest that plants with decreased chloroplast coverage in their BS cells have impaired $CO_2$ assimilation rates and PSII efficiency.

### Activities of Photosynthetic Enzymes Are Largely Unchanged in Complemented Lines

The decreased $CO_2$ assimilation in PEPC-BSD2 lines led us to measure in vitro enzyme activities of the key maize photosynthetic carboxylases and decarboxylase, as shown in Table II. No statistically significant differences were observed for Rubisco content (confirming the immunoblot analyses), Rubisco activity, or PEPC activity, except for the *bsd2* mutant. An increase in NADP-ME activity was observed in the homozygous PEPC-BSD2 line.

We also measured Rubisco activation status, and the ratio of Rubisco relative to key photosynthetic enzymes and stomatal conductance, to elucidate any other effect of altering BSD2 levels in the BS. Minor differences in Rubisco activation status were found; however, no differences were observed in the ratio of Rubisco relative to PEPC or NADP-ME (Table II). There also appeared to be a decrease in stomatal conductance in the hemizygous PEPC lines.

## DISCUSSION

In this study, we provide evidence for a previously unidentified function for the chloroplast chaperone BSD2. It has been well established that BSD2 is required for assembly of the Rubisco holoenzyme. The realization that it is equally present in maize M and BS chloroplasts (Friso et al., 2010), along with our own finding that a 50% decrease in BS BSD2 protein has no effect on Rubisco abundance, raised the possibility that the protein had additional functions. Our data support the conclusion that BSD2 has an ancillary role in BS cells related to chloroplast size, which, in turn, affects photosynthetic rate.

### Regulation of Chloroplast Number and Size

Chloroplast number is regulated through chloroplast division, which occurs via binary fission. A number of genes have been identified that promote or restrain chloroplast division (for review, see Osteryoung and Pyke, 2014). One early discovery for the *arc* (*accumulation and replication of chloroplast*) mutants was that their chloroplast coverage did not diverge from the wild type, indicating that the mechanisms that regulate chloroplast size and division are independent (Pyke and Leech, 1994). One protein recently identified as a regulator of chloroplast coverage is REDUCED CHLOROPLAST COVERAGE1, which is extraplastidic in localization (Larkin et al., 2016). One possibility is that BSD2 acts as a plastid-localized partner for signaling by a system, still uncharacterized, that involves REC1.

Characterization of complemented *bsd2* plants with constructs conferring high (UBI-BSD2 or RBCS-BSD2) or reduced (PEPC-BSD2) BSD2 expression in the BS revealed that overexpression increases chloroplast area and reduced expression decreases area. We considered that TEM analysis may have underestimated the chloroplast area due to dehydration of the tissue during fixation and embedding. Since this could potentially unequally affect perceived chloroplast and BS cell size, we used confocal imaging of live tissue as the main method to quantify chloroplast coverage. It is unlikely that BSD2 is involved directly in chloroplast division, since the number of chloroplasts per BS cell area did not vary (Fig. 4B).

**Table I.** *Maximum photochemical efficiency of PSII*

Data represent average $F_v/F_m$ ratio values of at least three complemented *bsd2* plants at PAR of zero ± SE. Statistical significance tests were conducted using a one-way ANOVA (*$P > 0.05$). NM, Not measured.

| Replicate | Wild Type | UBI | RBCS | PEPC (H) | PEPC (h) | *bsd2* Mutant |
|---|---|---|---|---|---|---|
| 1 | 0.759 ± 0.012 | 0.709 ± 0.037 | 0.753 ± 0.015 | 0.695 ± 0.039 | NM | 0.25 ± 0.030* |
| 2 | 0.829 ± 0.003 | 0.822 ± 0.001 | 0.807 ± 0.005 | 0.811 ± 0.002 | 0.816 ± 0.002 | 0.29 ± 0.021* |

In the transgenic lines, altered BSD2 content affected BS but not M chloroplasts, whether BSD2 was completely absent in the M (RBCS-BSD2) or overexpressed (PEPC-BSD2 and UBI-BSD2). A decoupling of chloroplast development between BS and M cells has been observed previously in $C_4$ plants, while the opposite has been observed in $C_3$ plants, best studied in reticulate mutants (Lundquist et al., 2014). These mutants typically have metabolic defects in BS chloroplasts that lead to a failure to signal M cells for normal chloroplast development. On the other hand, the *bsd1*/GOLDEN2 (Langdale and Kidner, 1994; Hall et al., 1998) and *bsd2* maize mutants have BS but not M chloroplast defects. GOLDEN2 encodes a transcription factor that is a member of a family with a conserved role in chloroplast development (Chen et al., 2016), and BSD2 is a zinc finger chaperone-type protein. It is possible that they represent elements of a poorly characterized network that is responsible for BS chloroplast development and, like reticulate mutants that affect both primary metabolism and M chloroplast development, have multiple functions, at least in the case of BSD2. Thus, our results suggest the possibility of an additional link between primary metabolism (i.e. carbon fixation) and chloroplast development, in this case in BS cells.

Dual functions of BSD2, which is an incomplete DnaJ protein, would be compatible with its chaperone motifs. True chloroplast DnaJ proteins have been characterized in *C. reinhardtii* (Willmund et al., 2008) and tomato (*Solanum lycopersicum*; Wang et al., 2015), where it appears to have a role protecting Rubisco under heat stress. Chloroplast DnaJ proteins comprise a gene family (Chiu et al., 2013), and if BSD2 is indeed a cochaperone akin to DnaJ, it could readily be imagined to be involved in folding and assembling Rubisco LS as well as folding, stabilizing, or assembling some other factor(s) that is involved in chloroplast division or size control. Our results suggest that such functions are hierarchical, since Rubisco abundance is unaffected at BSD2 levels that fail to support normal chloroplast coverage.

### Relationship of Chloroplast Volume and Photosynthesis

The relationship of chloroplast coverage to photosynthetic capacity has been poorly explored. Black and Mollenhauer (1971) proposed that the photosynthetic capacity of a plant is related to the quantity and coverage of leaf cellular organelles rather than their size, since a feature of plants with high photosynthetic capacity is a dense concentration of chloroplasts in the BS. It is now known that the high-photosynthetic-capacity plants they were observing were $C_4$ plants and their low-photosynthetic-capacity controls were $C_3$ species. Since the study compares $C_3$ and $C_4$ plants, the main cause of higher photosynthetic rates was most likely the high concentration of $CO_2$ around Rubisco. However, it is still unknown how much of a role chloroplast density in the BS may have on photosynthetic rates. We showed through gas exchange that the PEPC-BSD2 lines had decreased photosynthetic rates, correlated with reduced chloroplast coverage (Fig. 5). The precise mechanism, however, is still uncertain. Evidence points toward another deficit in photosynthesis that needs to be further explored. We can interpret the decreased photosynthetic rates in the PEPC-BSD2 lines as resulting from limited space (volume) for some component(s) of the photosynthetic machinery, leading to a possible deficit in electron transport capacity.

Additionally, reduced chloroplast coverage in the PEPC-BSD2 lines, which contain wild-type amounts of Rubisco, would predict that their chloroplasts are more densely packed with Rubisco and perhaps other photosynthetic machinery. It is possible that this could create physical or metabolite diffusion limitations that could negatively affect photosynthesis. Here, the PEPC-BSD2 lines appear to have increased resistance to $CO_2$ diffusion correlating with

**Table II.** *Summary of leaf gas exchange and photosynthetic enzyme activity*

Data represent averages of at least three replicates ± SE. Statistical significance tests were conducted using a one-way ANOVA (*$P > 0.05$). NM, Not measured.

| Parameter | Wild Type | UBI | RBCS | PEPC (H) | PEPC (h) | *bsd2* Mutant |
|---|---|---|---|---|---|---|
| Rubisco content ($\mu$mol catalytic sites $m^{-2}$) | 9.6 ± 1 | 9.3 ± 0.9 | 8.1 ± 1 | 9.2 ± 0.7 | NM | 0.47 ± 0.2 |
| Rubisco activity ($\mu$mol $CO_2$ $m^{-2}$ $s^{-1}$) | 31.3 ± 6 | 26.3 ± 6 | 26.7 ± 6 | 31.0 ± 2 | NM | 1.08 |
| PEPC activity ($\mu$mol $CO_2$ $m^{-2}$ $s^{-1}$) | 165.1 ± 30 | 151.5 ± 17 | 135.1 ± 2 | 150.7 ± 9 | NM | 141.25 |
| NADP-ME activity ($\mu$mol $CO_2$ $m^{-2}$ $s^{-1}$) | 74.4 ± 5 | 85.8 ± 8 | 71.8 ± 9 | 108.6 ± 6* | NM | 54.86 |
| PEPC:Rubisco | 5.8 ± 2 | 5.0 ± 1 | 5.4 ± 1 | 4.6 ± 0.6 | NM | 130.6 |
| NADP-ME:Rubisco | 2.8 ± 0.7 | 2.7 ± 0.3 | 2.8 ± 0.3 | 3.3 ± 0.05 | NM | 50.7 |
| Rubisco activation status | 75.5 ± 4 | 92.0 ± 11 | 72.7 ± 18 | 84.4 ± 4 | NM | NM |
| Stomatal conductance | 0.319 ± 0.003 | 0.233 ± 0.009 | 0.366 ± 0.02 | 0.212 ± 0.01 | 0.167 ± 0.007 | NM |

reduced photosynthetic rates, as indicated by maximum $C_i$ values around 800 $\mu$mol mol$^{-1}$ (300 $\mu$mol mol$^{-1}$ less than the wild type). The PEPC-BSD2 lines also have lower intercellular $CO_2$-to-ambient $CO_2$ ratio values than the wild type. Rubisco content, activity, and activation did not vary significantly between the complemented lines and wild-type plants. As a result, the functionality of Rubisco does not appear to contribute to the decreased photosynthetic rates observed.

Increased chloroplast coverage did not increase photosynthesis, suggesting that Rubisco abundance or activity, rather than chloroplast coverage, is limiting gains in $CO_2$ assimilation in excess of the wild type. Providing increased Rubisco in the context of greater chloroplast volume could test this hypothesis. In rice (*Oryza sativa*), contrasting results were found with regard to chloroplast size, where leaves with similar Rubisco content but different chloroplast size showed higher $CO_2$ assimilation with smaller chloroplasts. The authors concluded that the smaller chloroplasts conferred better $CO_2$ diffusion properties (Li et al., 2013). Additionally, it was reported recently in another $C_3$ plant that the larger, fewer chloroplasts in Arabidopsis (*Arabidopsis thaliana*) *arc* mutants result in decreased photosynthetic rates due to changes in $CO_2$ diffusion conductance in the M (Xiong et al., 2017). The types of correlations that can be made between chloroplast size, photosynthesis, and $CO_2$ diffusion in $C_4$ plants have yet to be determined.

## CONCLUSION

Complementation of the *bsd2* mutant has provided an opportunity to observe the effect of altered BSD2 expression in maize M and BS cells. The loss of BSD2 in the M has no observable effect on the plant; therefore, its role in the M remains unclear. Subjecting RBCS-BSD2 plants to heat stress, where chloroplast chaperones have important functions (Trösch et al., 2015), could uncover a role for BSD2 in this cell type. A 50% reduction of BSD2 in the BS, on the other hand, influenced chloroplast coverage and $CO_2$ assimilation but not Rubisco assembly. This suggests that BSD2 is likely present in excess of what is required for Rubisco assembly. Thus, we conclude that BSD2's primary function is Rubisco assembly in the BS and, secondarily, to regulate and maintain chloroplast size. Further studies of how BSD2 impacts chloroplast development could help develop approaches to manipulate chloroplast size. This could be particularly useful in engineering $C_4$ photosynthesis in $C_3$ plants (Stata et al., 2014). Manipulating chloroplast size also could lead to capturing greater photosynthetic efficiency by combining increased chloroplast coverage with increased RuBP regeneration and more efficient Rubisco.

## MATERIALS AND METHODS

### Construct Generation and Maize Transformation

Three expression cassettes containing different cell type-specific maize (*Zea mays*) promoters, the maize *BSD2* open reading frame, and the *Nos* terminator were assembled into pGEM T-Easy. Each construct was then stably transformed into Hi-II maize, a hybrid between inbreds A188 and B73. Maize transformation was carried out as described (Sattarzadeh et al., 2010). *BSD2* was commercially synthesized to encode the FLAG epitope at the 3′ end and inserted into pMK-RQ (Geneart, Fisher Scientific). All constructs contain the 272-bp *Nos* terminator amplified from the plasmid pHCnos (Wostrikoff et al., 2012). The binary vector pPTN 1055, referred to as PEPC-BSD2, contains the 1.7-kb maize PEPC promoter from the binary vector pPTN 512 (Sattarzadeh et al., 2010). UBI-BSD2 (binary vector pPTN 1052) contains the maize *UBI* promoter from pUbiHCnos (Wostrikoff et al., 2012), and RBCS-BSD2 or pPTN 1053 contains the maize RBCS1 promoter from the binary vector pPTN 533 (Sattarzadeh et al., 2010). T1 transgenic progeny were identified, and expression was determined for two independent, single-insertion events, from each of the three vectors, received from the University of Nebraska-Lincoln, using immunoblot analysis and the anti-FLAG antibody (Sigma-Aldrich). Details of the transgenic lines used are given in Supplemental Table S2.

### Plant Materials and Growth Conditions

Plants were grown in a greenhouse under a long-day cycle, 16-h/28°C days and 8-h/26°C nights. To eliminate endogenous *BSD2* expression, a representative event for each construct was crossed to a *BSD2/bsd2* heterozygote, since homozygous *bsd2* is seedling lethal. F1 progeny were genotyped for the transgene and *BSD2*. *BSD2/bsd2* heterozygotes that possessed the transgene were selfed to determine whether the transgene would complement the *bsd2* mutation. These F2 progeny segregated pale-green/seedling-lethal and wild-type-appearing plants. The wild-type-like plants were genotyped for *BSD2* using PCR (primers are given in Supplemental Table S1), and those determined to be *bsd2* homozygous mutants were assumed to be complemented. This was verified by genotyping for the transgene. The complemented plants were then selfed to obtain seed stocks homozygous for both the transgene and the *bsd2* mutation. Selected data for additional transgenic events obtained the same way are shown in Supplemental Figures S3, S6, and S7.

### RNA Characterization

Total RNA was extracted using Tri reagent (Molecular Research Center), and 1 to 5 $\mu$g was analyzed by gel-blot hybridization at 65°C using the buffer of Church and Gilbert (1984). *BSD2*, *rbcL*, and *psbA* probes were generated by PCR using the primers shown in Supplemental Table S1.

### Protein Characterization

Total leaf protein was extracted on a leaf area basis (two- to four-hole punches of leaf tissue) from the tip of the third leaf as described (Barkan, 1998). Protein was separated through 13% SDS-polyacrylamide gels and blotted onto polyvinylidene difluoride membranes (Bio-Rad). Primary antibodies were incubated overnight at 4°C in TBS plus 0.1% Tween 20. Antibodies used were anti-LS (Agrisera), anti-ME (a kind gift of Dr. Timothy Nelson), anti-PEPC (Agrisera), anti-FLAG (Sigma-Aldrich), and anti-BSD2 (Feiz et al., 2014). Incubation with goat anti-rabbit IR dye 800 CW (LI-COR) secondary antibody was performed at room temperature for 2 h, and blots were imaged using the LI-COR Odyssey Infrared Imaging System. Gels that were not blotted were stained with 0.01% Coomassie Blue R-250 and also imaged using the Odyssey system.

### M/BS Extraction

BS and M extractions were performed using 1 to 2 g of leaves as described (Markelz et al., 2003), except that BS isolation was carried out entirely at 4°C to minimize degradation. RNA and protein were then isolated from the M and BS extracts as described above.

### TEM

Observation of chloroplast ultrastructure by TEM was performed as described previously (Zhang et al., 2012). Fully developed leaves (2-week-old third leaves) were used. Pieces of 1 × 1 mm were excised, fixed in 2% (w/v) paraformaldehyde and 2% (v/v) glutaraldehyde in 0.05 M cacodylic acid buffer, pH 7.4, and postfixed in 2% (v/v) osmium tetroxide in the same buffer at 4°C for 3 h. Samples were dehydrated subsequently with a graded series (50%, 70%,

90%, and 100%) of ethanol. The samples were infiltrated by propylene oxide twice for 30 min and placed into a 70:30 mixture of propylene oxide and resin (Quetol-651; Nisshin EM) for 1 h. Ethanol was finally replaced with resin, and the samples were polymerized at 60°C for 48 h. The chloroplast structures were evaluated on ultrathin sections using an ultramicrotome (Ultracut UCT; Leica). Sections were stained with 2% uranyl acetate and were examined using a transmission electron microscope (JEM-1200EX; JEOL) at 80 kV. Microscopic observations were conducted at Tokai Electron Microscopy.

## Confocal Microscopy

Leaf sections of 2-week-old plants were prepared manually with a razor blade. Images were collected at the BTI Plant Cell Imaging Center on a Leica TCS-SP5 confocal microscope (Leica Microsystems) using a 63× water-immersion objective with numerical aperture 1.2 and zoom 1.6. Chloroplasts were excited with the blue argon laser (488 nm), and emitted light was collected from 500 to 550 nm. Differential interference contrast images were collected simultaneously with the fluorescence images using the transmitted light detector. Images were processed using Leica LAS-AF software (version 2.6.0) and Adobe Photoshop CS2 version 9.0.2 (Adobe Systems). Chloroplast area was obtained by outlining only areas covered by chloroplasts in each BS cell, while BS cell area was obtained by outlining the outer edge of each BS cell. This was done for both confocal and TEM images, which were quantified using ImageJ.

## Leaf Gas-Exchange Measurements

Gas-exchange measurements were carried out on the youngest fully expanded leaf of 2- to 3-week-old plants using the LI-COR 6400 portable open photosynthesis system. Each leaf was given 2 to 3 min to reach the steady state of $CO_2$ uptake in the chamber before measurements were taken. Relative humidity was kept near 60%. Photosynthetic responses were measured at 12 light intensities at 400 $\mu$L $L^{-1}$ $CO_2$ and 25°C. Photosynthetic responses to intercellular $CO_2$ concentration ($A/C_i$ curves) were measured at 16 $CO_2$ steps at saturating light intensity of 1,800 $\mu$mol $m^{-2}$ $s^{-1}$ and 25°C.

## Chlorophyll Fluorescence Imaging

Chlorophyll fluorescence was measured by Monitoring-PAM (Heinz Walz) at room temperature. Leaves attached to 2-week-old plants grown in the greenhouse (second from the top) were subjected to dark adaptation for at least 15 min prior to chlorophyll fluorescence measurement. $F_v/F_m$ was calculated as $(F_m - F_o)/F_m$, where $F_m$ is the maximum fluorescence level and $F_o$ is the minimum fluorescence level under the measuring light. ΦPSII was calculated as $(F_m' - F_s)/F_m'$, where $F_m'$ is the maximum fluorescence level and $F_s$ is the steady-state fluorescence level under the actinic light. NPQ was calculated as $(F_m - F_m')/F_m'$.

## Leaf Protein Extraction and Rubisco Activation and Content Measurements

Leaf samples (0.5 $cm^2$) were frozen in liquid nitrogen and stored at −80°C. Soluble leaf protein was extracted into 1 mL of ice-cold, $N_2$-sparged extraction buffer [50 mM EPPS-NaOH, pH 8, 0.5 mM EDTA, 2 mM DTT, 1% (v/v) plant protease inhibitor cocktail (Sigma-Aldrich), and 1% (w/v) PVPP)] with 5 mM $MgCl_2$ using 2-mL glass homogenizers (Wheaton; Sharwood et al., 2016). The lysate was centrifuged for 30 s (16,000*g*, 4°C), and 10 $\mu$L of the soluble protein was assayed for initial and total Rubisco activities using an NADH-coupled enzyme method at 25°C (Lilley et al., 1975; Sharwood et al., 2016). To measure initial Rubisco activity, RuBP (0.4 mM) was added to the buffer prior to the addition of extract (10 $\mu$L) to start the assay. Total Rubisco activity was determined after Rubisco in the leaf protein was activated for 10 min in assay buffer before initiating Rubisco activity measurements by adding RuBP to 0.4 mM. The RuBP used in the assays was synthesized and purified as described previously (Kane et al., 1998). Rubisco content was determined in 100 $\mu$L of soluble extract by [$^{14}$C]CABP binding (Sharwood et al., 2008). Soluble protein content was determined by the Coomassie dye-bind assay (Pierce) using BSA standards.

## PEPC and NADP-ME Activities

Total PEPC activities in leaf extracts were measured using an NADH-coupled assay as described previously (Ashton et al., 1990; Sharwood et al., 2014). Extraction was performed using the same buffer as described above. Total NADP-ME activity was determined in a coupled NADP assay as described previously (Ashton et al., 1990; Pengelly et al., 2012).

## Statistical Analysis

Jmp pro 13 software was used to determine the statistical significance of the differences observed between the nontransgenic controls and transgenic plants. One way Tukey-Kramer HSD ANOVA tests were performed ($P < 0.05$).

## Supplemental Data

The following supplemental materials are available.

**Supplemental Figure S1.** Validation of complementation for lines used in the experiments.

**Supplemental Figure S2.** Replicate blots of BSD2 protein accumulation and cell specificity in transgenic lines.

**Supplemental Figure S3.** Protein accumulation from two transgenic events.

**Supplemental Figure S4.** *rbcL* transcript accumulation and cell specificity in *bsd2* complemented plants.

**Supplemental Figure S5.** Confocal microscopy images from 2-week-old leaf tip tissue.

**Supplemental Figure S6.** Quantification of chloroplast coverage in BS cells.

**Supplemental Figure S7.** $CO_2$ assimilation measurements with varying $C_i$.

**Supplemental Table S1.** Primers used in this work.

**Supplemental Table S2.** Transgenic lines used in this work.

## ACKNOWLEDGMENTS

We thank Tom Clemente (University of Nebraska-Lincoln) for designing strategies to assemble transformation constructs and Shirley Sato (University of Nebraska-Lincoln) for assembling the constructs, conducting maize transformations, and providing seed from T0 lines. Dr. Tim Nelson (Yale University) is thanked for sharing ME antibody. We also thank Florian Busch (Australian National University) for helpful technical discussions, Tsuneaki Takami (Okayama University) for technical assistance in gas exchange and chlorophyll fluorescence, and the BTI Plant Cell Imaging Center for assistance in confocal microscopy.

Received September 18, 2017; accepted October 27, 2017; published October 31, 2017.

## LITERATURE CITED

**Ashton AR, Burnell JN, Furbank RT, Jenkins CLD, Hatch MD** (1990) Enzymes of $C_4$ photosynthesis. *In* PJ Lea, ed, Methods in Plant Biochemistry. Academic Press, London, pp 39–71

**Barkan A** (1998) Approaches to investigating nuclear genes that function in chloroplast biogenesis in land plants. Methods Enzymol **297:** 38–57

**Black CC, Mollenhauer HH** (1971) Structure and distribution of chloroplasts and other organelles in leaves with various rates of photosynthesis. Plant Physiol **47:** 15–23

**Brutnell TP, Sawers RJ, Mant A, Langdale JA** (1999) BUNDLE SHEATH DEFECTIVE2, a novel protein required for post-translational regulation of the *rbcL* gene of maize. Plant Cell **11:** 849–864

**Chen M, Ji M, Wen B, Liu L, Li S, Chen X, Gao D, Li L** (2016) GOLDEN 2-LIKE transcription factors of plants. Front Plant Sci **7:** 1509

**Chiu CC, Chen LJ, Su PH, Li HM** (2013) Evolution of chloroplast J proteins. PLoS ONE **8:** e70384

**Choquet Y, Wollman FA** (2009) The CES process. Chlamydomonas Sourcebook **2:** 1027–1063

**Church GM, Gilbert W** (1984) Genomic sequencing. Proc Natl Acad Sci USA **81:** 1991–1995

**Doron L, Segal N, Gibori H, Shapira M** (2014) The BSD2 ortholog in *Chlamydomonas reinhardtii* is a polysome-associated chaperone that co-migrates on sucrose gradients with the rbcL transcript encoding the Rubisco large subunit. Plant J **80:** 345–355

**Feiz L, Williams-Carrier R, Belcher S, Montano M, Barkan A, Stern DB** (2014) A protein with an inactive pterin-4a-carbinolamine dehydratase domain is required for Rubisco biogenesis in plants. Plant J **80:** 862–869

**Feiz L, Williams-Carrier R, Wostrikoff K, Belcher S, Barkan A, Stern DB** (2012) Ribulose-1,5-bis-phosphate carboxylase/oxygenase accumulation factor1 is required for holoenzyme assembly in maize. Plant Cell **24:** 3435–3446

**Friso G, Majeran W, Huang M, Sun Q, van Wijk KJ** (2010) Reconstruction of metabolic pathways, protein expression, and homeostasis machineries across maize bundle sheath and mesophyll chloroplasts: large-scale quantitative proteomics using the first maize genome assembly. Plant Physiol **152:** 1219–1250

**Hall LN, Rossini L, Cribb L, Langdale JA** (1998) GOLDEN 2: a novel transcriptional regulator of cellular differentiation in the maize leaf. Plant Cell **10:** 925–936

**Kane HJ, Wilkin JM, Portis AR, Andrews TJ** (1998) Potent inhibition of ribulose-bisphosphate carboxylase by an oxidized impurity in ribulose-1,5-bisphosphate. Plant Physiol **117:** 1059–1069

**Kramer DM, Evans JR** (2011) The importance of energy balance in improving photosynthetic productivity. Plant Physiol **155:** 70–78

**Langdale JA, Kidner CA** (1994) *bundle sheath defective*, a mutation that disrupts cellular differentiation in maize leaves. Development **120:** 673–681

**Larkin RM, Stefano G, Ruckle ME, Stavoe AK, Sinkler CA, Brandizzi F, Malmstrom CM, Osteryoung KW** (2016) REDUCED CHLOROPLAST COVERAGE genes from *Arabidopsis thaliana* help to establish the size of the chloroplast compartment. Proc Natl Acad Sci USA **113:** E1116–E1125

**Li Y, Ren B, Ding L, Shen Q, Peng S, Guo S** (2013) Does chloroplast size influence photosynthetic nitrogen use efficiency? PLoS ONE **8:** e62036

**Lilley RM, Fitzgerald MP, Rienits KG, Walker DA** (1975) Criteria of intactness and the photosynthetic activity of spinach chloroplast preparations. New Phytol **75:** 1–10

**Lundquist PK, Rosar C, Bräutigam A, Weber AP** (2014) Plastid signals and the bundle sheath: mesophyll development in reticulate mutants. Mol Plant **7:** 14–29

**Markelz NH, Costich DE, Brutnell TP** (2003) Photomorphogenic responses in maize seedling development. Plant Physiol **133:** 1578–1591

**Maxwell K, Johnson GN** (2000) Chlorophyll fluorescence: a practical guide. J Exp Bot **51:** 659–668

**Osteryoung KW, Pyke KA** (2014) Division and dynamic morphology of plastids. Annu Rev Plant Biol **65:** 443–472

**Pengelly JJ, Tan J, Furbank RT, von Caemmerer S** (2012) Antisense reduction of NADP-malic enzyme in *Flaveria bidentis* reduces flow of $CO_2$ through the $C_4$ cycle. Plant Physiol **160:** 1070–1080

**Pyke KA, Leech RM** (1994) A genetic analysis of chloroplast division and expansion in *Arabidopsis thaliana*. Plant Physiol **104:** 201–207

**Roth R, Hall LN, Brutnell TP, Langdale JA** (1996) *bundle sheath defective2*, a mutation that disrupts the coordinated development of bundle sheath and mesophyll cells in the maize leaf. Plant Cell **8:** 915–927

**Sattarzadeh A, Fuller J, Moguel S, Wostrikoff K, Sato S, Covshoff S, Clemente T, Hanson M, Stern DB** (2010) Transgenic maize lines with cell-type specific expression of fluorescent proteins in plastids. Plant Biotechnol J **8:** 112–125

**Sharwood RE, Sonawane BV, Ghannoum O** (2014) Photosynthetic flexibility in maize exposed to salinity and shade. J Exp Bot **65:** 3715–3724

**Sharwood RE, Sonawane BV, Ghannoum O, Whitney SM** (2016) Improved analysis of C4 and C3 photosynthesis via refined *in vitro* assays of their carbon fixation biochemistry. J Exp Bot **67:** 3137–3148

**Sharwood RE, von Caemmerer S, Maliga P, Whitney SM** (2008) The catalytic properties of hybrid Rubisco comprising tobacco small and sunflower large subunits mirror the kinetically equivalent source Rubiscos and can support tobacco growth. Plant Physiol **146:** 83–96

**Stata M, Sage TL, Rennie TD, Khoshravesh R, Sultmanis S, Khaikin Y, Ludwig M, Sage RF** (2014) Mesophyll cells of C4 plants have fewer chloroplasts than those of closely related C3 plants. Plant Cell Environ **37:** 2587–2600

**Trösch R, Mühlhaus T, Schroda M, Willmund F** (2015) ATP-dependent molecular chaperones in plastids: more complex than expected. Biochim Biophys Acta **1847:** 872–888

**Wang G, Kong F, Zhang S, Meng X, Wang Y, Meng Q** (2015) A tomato chloroplast-targeted DnaJ protein protects Rubisco activity under heat stress. J Exp Bot **66:** 3027–3040

**Willmund F, Dorn KV, Schulz-Raffelt M, Schroda M** (2008) The chloroplast DnaJ homolog CDJ1 of *Chlamydomonas reinhardtii* is part of a multichaperone complex containing HSP70B, CGE1, and HSP90C. Plant Physiol **148:** 2070–2082

**Wostrikoff K, Clark A, Sato S, Clemente T, Stern D** (2012) Ectopic expression of Rubisco subunits in maize mesophyll cells does not overcome barriers to cell type-specific accumulation. Plant Physiol **160:** 419–432

**Wostrikoff K, Stern D** (2007) Rubisco large-subunit translation is autoregulated in response to its assembly state in tobacco chloroplasts. Proc Natl Acad Sci USA **104:** 6466–6471

**Xiong D, Huang J, Peng S, Li Y** (2017) A few enlarged chloroplasts are less efficient in photosynthesis than a large population of small chloroplasts in *Arabidopsis thaliana*. Sci Rep **7:** 5782

**Zhang L, Kato Y, Otters S, Vothknecht UC, Sakamoto W** (2012) Essential role of VIPP1 in chloroplast envelope maintenance in *Arabidopsis*. Plant Cell **24:** 3695–3707